AIP | Journal of Applied Physics

Effect of gigaelectron volt Au-ion irradiation on the characteristics of ultrananocrystalline diamond films

Huang-Chin Chen, Kuang-Yau Teng, Chen-Yau Tang, Balakrishnan Sundaravel, Sankarakumar Amirthapandian, and I-Nan Lin

Citation: Journal of Applied Physics **108**, 123712 (2010); doi: 10.1063/1.3524541
View online: http://dx.doi.org/10.1063/1.3524541
View Table of Contents: http://scitation.aip.org/content/aip/journal/jap/108/12?ver=pdfcov
Published by the AIP Publishing

Effect of gigaelectron volt Au-ion irradiation on the characteristics of ultrananocrystalline diamond films

Huang-Chin Chen,[1] Kuang-Yau Teng,[1] Chen-Yau Tang,[1] Balakrishnan Sundaravel,[2] Sankarakumar Amirthapandian,[2,3] and I-Nan Lin[1,a)]
[1]*Department of Physics, Tamkang University, Tamsui, Taiwan 251, Republic of China*
[2]*Materials Science Group, Indira Gandhi Centre for Atomic Research, Kalpakkam 603102, India*
[3]*Institut für Halbleiteroptik und Funktionelle Grenzflächen, Universität Stuttgart, Allmandring 3, 70569 Stuttgart, Germany*

(Received 18 August 2010; accepted 4 November 2010; published online 29 December 2010)

The effect of 2.245 GeV Au-ion irradiation/postannealing processes on the electron field emission (EFE) properties of ultrananocrystalline diamond (UNCD) films was investigated. Au-ion irradiation with a fluence of around 8.4×10^{13} ions/cm^2 is required to induce a large improvement in the EFE properties of the UNCD films. Postannealing the Au-ion irradiated films at 1000 °C for 1 h slightly degraded the EFE properties of the films but the resulting EFE behavior was still markedly superior to that of pristine UNCD films. Transmission electron microscopy examinations revealed that the EFE properties of the UNCD films are primarily improved by Au-ion irradiation/postannealing processes because of the formation of nanographites along the trajectory of the irradiating ions, which results in an interconnected path for electron transport. In contrast, the induction of grain growth process due to Au-ion irradiation in UNCD films is presumed to insignificantly degrade the EFE properties for the films as the aggregates are scarcely distributed and do not block the electron conducting path. © *2010 American Institute of Physics*.
[doi:10.1063/1.3524541]

I. INTRODUCTION

Diamond films have been extensively investigated for their application as electron field emitters owing to their negative electron affinity and low effective work function.[1,2] While the physical properties depend on the crystallinity of the materials, the electrical and optical characteristics of the films are more closely related to the microstructure of the samples.[3] During the growth of diamond films, hydrogen is usually incorporated into the materials and is presumed to reside at the grain boundaries.[4] Studies have been conducted on the correlation of hydrogen retention with the bonding,[4–6] conductivity,[7] and field emission[8,9] of diamond films. However, the control of hydrogen content in the diamond films is complicated. On the other hand, the sp^2-bonded carbon within chemical vapor deposited (CVD) diamond films can be thought of as a conduction promoter, particularly if the sp^2-bonds form interconnected networks along which electrons are free to move.[4] Control of the proportion of sp^2-bonds can be achieved by the irradiation of energetic heavy ions into the diamond thin films. Many reports have discussed the effects of ion beam irradiation on the characteristics of type IIa diamond,[10] diamondlike carbon films,[11] taC,[12], graphite,[13] and polycrystalline CVD diamond films.[14–16] Furthermore, Pandey *et al.*[17] and Koinkar *et al.*[18] have studied the field emission enhancement by swift heavy ion irradiation in CVD diamonds but the mechanism is still not clear.

Here, we report on the effect of heavy-ion (2.245 GeV Au) irradiation in improving the electron field emission (EFE) properties of diamond films. The modifications in the microstructure of these films due to heavy ion irradiation were investigated in detail using transmission electron microscopy (TEM), and the correlation of these characteristics with the resulting EFE characteristics is discussed.

II. EXPERIMENTAL PROCEDURES

Ultrananocrystalline diamond (UNCD) films of ~300 nm thickness were deposited on silicon substrates by an Ar-plasma-based microwave plasma enhanced (MPECVD) process for 60 min using an IPLAS-cyrannus reactor. A gas mixture of CH_4 and Ar with flow rates of 1 SCCM and 99 SCCM, respectively, (SCCM denotes cubic centimeter per minute at STP) was excited by 1200 W microwave radiation at 2.45 GHz, and the total pressure in the chamber was maintained at 100 torr. The substrate temperature was estimated to be around 475 °C during the growth of the UNCD films. The diamond films were subjected to 2.245 GeV Au-ion irradiation from the universal linear accelerator (UNILAC) at GSI Helmholtzzentrum für Schwerionenforschung GmbH, Darmstadt, Germany, with fluences of 1×10^{11} to 8.4×10^{13} ions/cm^2. The pristine UNCD films were designated as $UNCD_I$, and those irradiated with medium-level ion fluences (1×10^{11}–5×10^{12} ions/cm^2) were designated as $UNCD_{II}$. The high-level ion fluence (8.4×10^{13} ions/cm^2) Au-ion-irradiated films were designated as $UNCD_{III}$ for as-irradiated films and as $UNCD_{IV}$ for irradiation/postannealed films. The postannealing process was conducted in a 5% H_2/Ar atmosphere at 1000 °C for 1 h. The 2.245 GeV gold ions have a projected range of 66.4 μm in diamond with longitudinal straggling of

a)Electronic mail: inanlin@mail.tku.edu.tw.

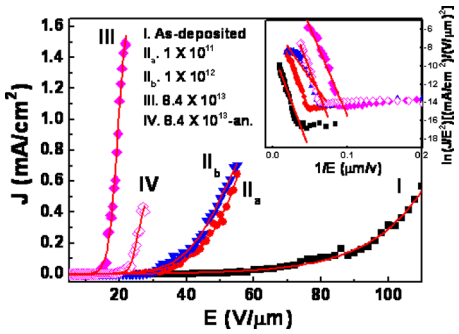

FIG. 1. (Color online) The EFE properties of UNCD samples: (I) pristine UNCD, (II) medium-level fluence ($1.0\times10^{11}-1\times10^{12}$ ions/cm^2) 2.245 GeV Au-ion irradiated, (III) high-level fluence (8.4×10^{13} ions/cm^2) Au-ion irradiated, and (IV) postannealed after Au-ion irradiation (2.245 GeV and 8.4×10^{13} ions/cm^2). The insets show the corresponding Fowler–Nordheim plots.

1.93 μm as simulated with SRIM-2008.[19] Therefore, the Au-ions will pass through the diamond films and get buried deep into the substrate for all the samples rather than residing inside the diamond films. The sole effect of heavy ion irradiation is to induce atomic defects in the UNCD films rather than acting as dopants. The Au-ions have an electronic energy loss of 3.338×10^4 eV/nm and a nuclear energy loss of 28.99 eV/nm, which indicates that the ions will lose energy mostly through electronic excitations in the diamond. The lattice damage effects of nuclear energy loss will be minimal.

The films were characterized using scanning electron microscopy (SEM: JEOL JSM-6500F), Raman spectroscopy (Renishaw, excitation wavelength=514.5 nm) and TEM (JEOL 2100). EFE properties of the diamond films were measured with a tunable parallel plate set-up in which the sample-to-anode distance was varied using a micrometer. The current density-electric field (J-E) characteristics were measured using an electrometer (Keithley 237) under pressures below 10^{-6} torr. The EFE parameters were extracted from the obtained J-E curves with the Fowler–Nordheim model[20] where the turn-on field was designated as the intersection of the lines extrapolated from the low field and high field segments of the Fowler–Nordheim plots.

III. RESULTS AND DISCUSSION

The pristine UNCD films ($UNCD_I$) are highly resistive and exhibit poor EFE properties. Curve I in Fig. 1 indicates that large fields ($E_0=30$ V/μm) are required to turn-on the EFE process. The Au-ion irradiation markedly improved the EFE properties of the UNCD films. Curves II_a and II_b (Fig. 1) show that the turn-on field decreased to around $E_0=19-20.5$ V/μm for the $UNCD_{II}$ films, which were irradiated with Au-ions at medium level ion fluences ($1\times10^{11}-1\times10^{12}$ ions/cm^2). This drop was accompanied by an increase in the EFE current density to around $J_e=0.7$ mA/cm^2 at a 58 V/μm applied field. Surprisingly, the EFE was enhanced drastically when the fluence for Au-ion irradiation increased to 8.4×10^{13} ions/cm^2 for $UNCD_{III}$ (curve III, Fig. 1). The turn-on field decreased to around $E_0=11.6$ V/μm, which was accompanied by an abrupt jump in the EFE current density to around $J_e=1.6$ mA/cm^2 at a 20 V/μm applied field, levels at which the pristine and medium-dosage-irradiated UNCD films are essentially non-emitting ($J_e<0.005$ mA/cm^2).

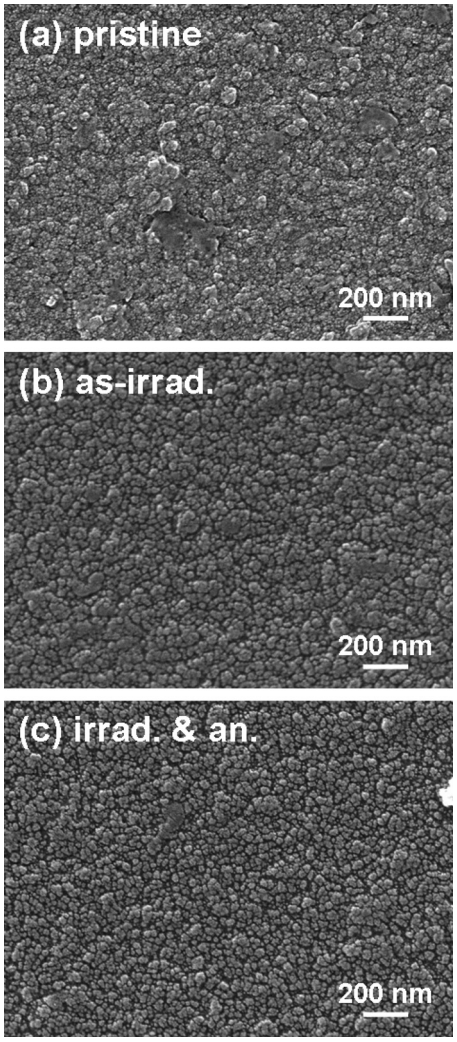

FIG. 2. SEM micrographs for the (a) pristine UNCD films, (b) high-level fluence (8.4×10^{13} ions/cm^2) Au-ion irradiated UNCD films, and (c) Au-ion irradiated/postannealed (2.245 GeV and 8.4×10^{13} ions/cm^2) UNCD films.

The SEM microstructures of the UNCD films are hardly altered by the Au-ion irradiation [Figs. 2(a) and 2(b)]. The Raman spectrum is also insignificantly modified by a medium-level fluence of Au-ion irradiation. All the Raman spectra (curves I, II_a, and II_b, Fig. 3) contain ν_1-band (1140 cm^{-1}) and ν_2-band (1480 cm^{-1}) resonance peaks, which correspond to transpolyacetylene at the grain boundaries,[21,22] and D*-band (1350 cm^{-1}) and G-band (1580 cm^{-1}) resonance peaks, which correspond to disordered carbons.[23,24] These Raman spectra are typical characteristic for UNCD films with ultrasmall grains. The D-band (1320 cm^{-1}) resonance peaks, which correspond to the T_{2g} resonance mode of the 3C diamond lattice, are only barely visible. In contrast, the Raman spectra are markedly altered due to the high-level fluence (8.4×10^{13} ions/cm^2) Au-ion irradiation. Curve III (Fig. 3) shows that all the resonance peaks corresponding to UNCD materials are diminished, replaced by noisy signals with a broadened peaks near G*

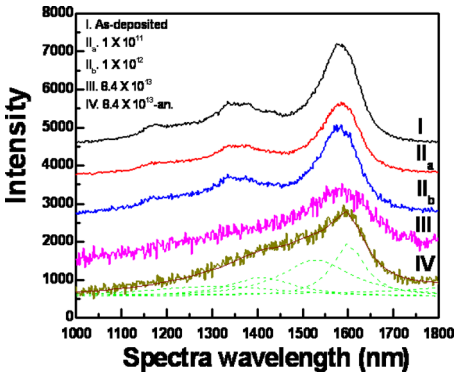

FIG. 3. (Color online) The Raman spectra of UNCD samples: (I) pristine UNCD, (II) medium-level fluence (1.0×10^{11}–1×10^{12} ions/cm^2) 2.245 GeV Au-ion irradiated, (III) high-level fluence (8.4×10^{13} ions/cm^2) Au-ion irradiated, and (IV) postannealed after Au-ion irradiation (2.4 GeV and 8.4×10^{13} ions/cm^2).

$=1580$ cm^{-1}, which characterize nanographites. This result infers that a large proportion of sp^2-bonds have been induced. The significance of such a phenomenon will be further discussed below. It should be noted that visible Raman spectroscopy is more than ten times more sensitive to sp^2-bonds than sp^3-bonds. An overwhelmingly larger sp^2-than sp^3-signal in Raman spectroscopy does not indicate that all the sp^3-bonded materials have been converted into sp^2-bonded materials.

To investigate the source of the enhancement of the EFE properties for UNCD films due to Au-ion irradiation, the microstructure of the UNCD films was examined in detail using TEM. Figure 4 shows that the pristine UNCD films contain ultrasmall grains of spherical geometry. Interestingly, the grains are uniformly small (~5 nm) with a very narrow size distribution. Lattice fringes in the structure image (inset, Fig. 4) reveal that the spacing between (111) planes is 0.205 nm, which is a typical value for diamond materials and confirms that these materials are diamond. The microstructure of the UNCD$_{III}$ films, which were irradiated with Au-ions at 8.4×10^{13} ions/cm^2, is shown in Fig. 5. A typical bright field (BF) TEM image of the UNCD$_{III}$ films, shown in Fig. 5(a), indicates the presence of large aggregates around 80 $\times$80 nm in size. The large aggregates are scarcely distributed over the samples. The inset in Fig. 5(a) reveals that the selected area electron diffraction pattern (SAED) contains only the ring-shaped pattern, which implies that most of the material is still randomly oriented nanodiamond grains. There also exists a prominent diffused ring in the center of this SAED, which indicates the existence of some amorphous carbons (or graphites) in these films and is in accord with the observation of Raman spectroscopy (cf. Fig. 3). Dark field (DF) images, which were taken using a (0002) graphite diffraction spot as indicated in SAED [green circle, inset, Fig. 5(a)] are shown in Fig. 5(b) and reveal that, in addition to the crystals corresponding to large aggregates (orange color) and nanosized diamonds (blue color), there exist numerous tiny spots (green color) corresponding to graphites. The nanosized graphites are uniformly distributed over the samples. A linear diffraction pattern (ldp_1, curve I in Fig. 6) extracted from SAED more clearly indicates that some graphite signals appear in addition to the large background that represents the amorphous phase. The significance of the presence of amorphous carbons (or graphites) will be discussed shortly.

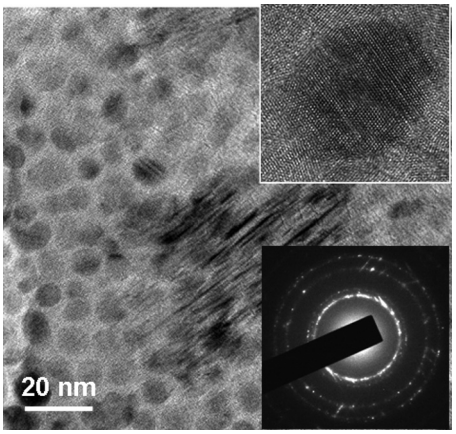

FIG. 4. TEM micrographs for pristine UNCD films with insets showing the SAED of the samples and a structure image of typical diamond grains.

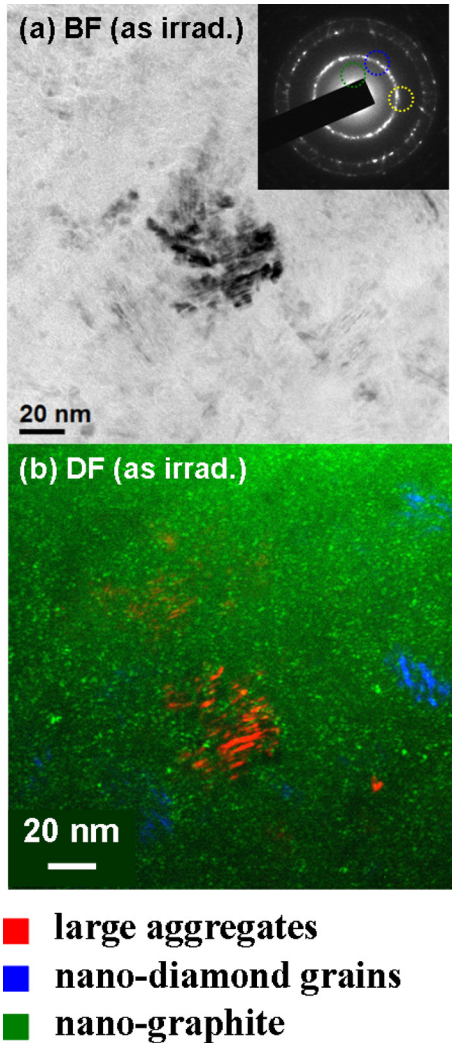

FIG. 5. (Color online) (a) BF and (b) DF TEM micrographs for UNCD films as-irradiated with 2.245 GeV Au-ions (8.4×10^{13} ions/cm^2). The inset in (a) shows the SAED of the corresponding samples.

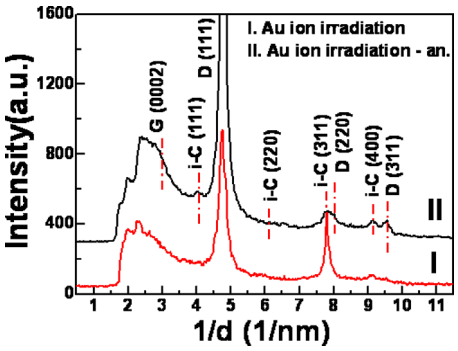

FIG. 6. (Color online) The linear diffraction pattern (*ldp*) of UNCD samples extracted from the corresponding SAED (I) as-irradiated with 2.245 GeV Au-ions (8.4×10^{13} ions/cm^2) and (II) postannealed at 1000 °C (1 h) after Au-ion irradiation.

Figure 7(a) shows that the large aggregates in as-irradiated ($UNCD_{III}$) films contain small clusters about 10–15 nm in size, which are about two to three times as large as the grain size of pristine UNCD films. The grain growth process has been induced due to Au-ion irradiation. Fourier-transformed (FT) diffractograms corresponding to the whole region in Fig. 7(a) [inset "0," Fig. 7(a)] indicate that the clusters in this aggregate are oriented nearly along the same direction, i.e., the 101 zone axis. All the clusters contain parallel fringes. There are streaks (rel-rods) along the 111 direction associated with each major diffraction spot, which indicates that the clusters in the aggregates contain (111) planar defects, most probably as stacking faults.[25] The presence of defects in the clusters is further demonstrated by the FT diffractograms FT_1 and FT_2 corresponding to the areas 1 and 2 designated in Fig. 7(a), respectively, again revealing that the clusters are oriented along the 101 zone axis and are heavily faulted (i.e., contain streaks).

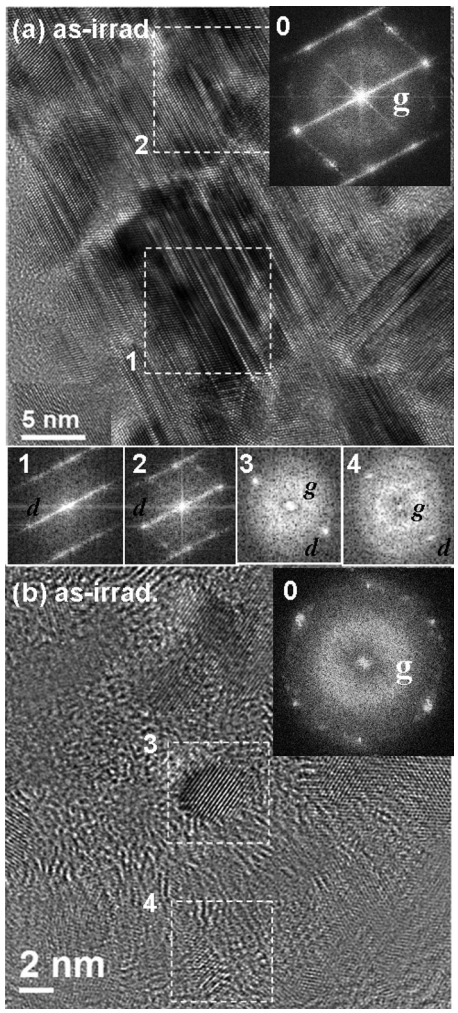

FIG. 7. TEM structure images for UNCD films as-irradiated with 2.245 GeV Au-ions (8.4×10^{13} ions/cm^2); (a) typical large-aggregates region and (b) small-grain region along with the FT diffractograms (FT_0) of the corresponding region (insets FT_1–FT_4 show, respectively, the FT diffractograms of the designated areas 1–4 in "a" and "b").

In contrast, the structure image corresponding to the small-grain region in $UNCD_{III}$ films is shown in Fig. 7(b). The associated FT-diffractogram (FT_0) for the whole region in Fig. 7(b) is shown in the inset and indicates that there exists a nanographite (or amorphous carbon) phase (diffused ring, FT_0) along with the ultrasmall diamond grains (spotty pattern, FT_0). The presence of ultrasmall diamond grains is further demonstrated in area 3 and the FT_3 diffractogram whereas the existence of nanographites (or amorphous carbons) is demonstrated in area 4 and the FT_4 diffractograms. It should be noted that the diffused ring is also observed in FT_0 of the large-grain region [cf. Fig. 7(a)] but it is lower in intensity and is presumed to be contributed by the nanographites underneath the large diamond grains rather than inside them. Restated, the nanographites are possibly locating either along the UNCD grain boundaries or between the interface regions of large diamond aggregates and UNCD grains. The presence of nanographites may form an interconnected conduction path for electrons that thereafter enhances the EFE process. Presumably, the nanographites can be formed only when the incident ions are energetic and are of large enough fluence to induce the melting and recrystallization process for amorphous carbons in the diamond films along the trajectory of the irradiated ions.

Postannealing of the Au-ion irradiated films at 1000 °C (1 h) insignificantly modified the SEM morphology of the samples [Fig. 2(c)]. The Raman spectra were only moderately modified, i.e., the Raman signal is still noisy and contains only the G-band resonance peak at 1580 cm^{-1} (curve IV, Fig. 3). The G-band resonance peak is slightly narrower. Such a postannealing process moderately degrades the EFE properties of the 8.4×10^{13} ions/cm^2 Au-ion irradiated films. Figure 1 (curve IV) shows that the turn-on field increased slightly to around $(E_0)_{IV}=13.5$ V/μm, and the EFE current density decreased slightly to around $(J_e)_{IV}=0.4$ mA/cm^2 at a 28 V/μm applied field compared with $(E_0)_{III}=11.2$ V/μm and $(J_e)_{III}=1.5$ mA/cm^2 (at 28 V/μm) for the as-irradiated films (cf. curve III, Fig. 1). Interestingly, analyses on these J-E curves using the Fowler–Nordheim model indicated that all the as-irradiated or irradiated/annealed films possess similar effective work functions $\phi_e=\phi^{3/2}/\beta$ where ϕ is the work function of the materials and β is the field enhancement factor of the emission sites. The ϕ_e-value is around 0.28–0.32, which corresponds to $\beta=350-399$ when $\phi=5.1$ eV was assumed for diamond materials. These results imply that the modification on the EFE

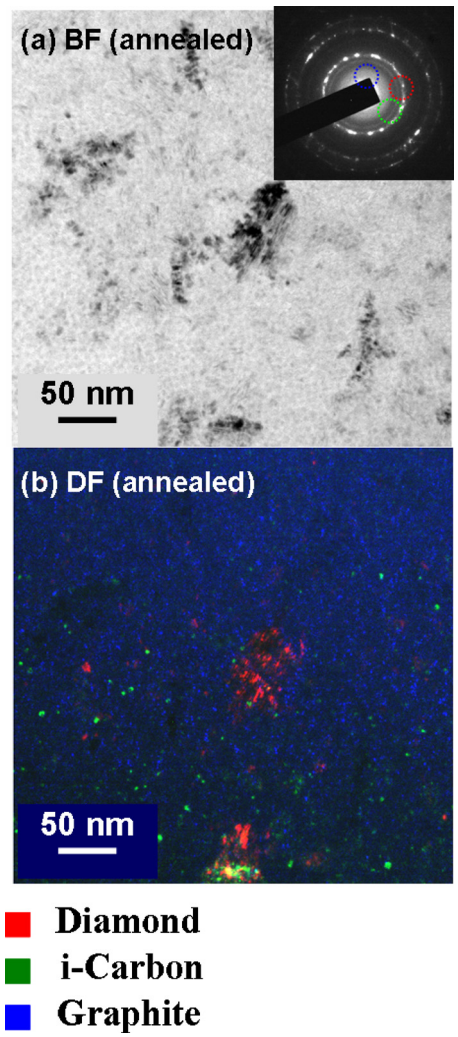

FIG. 8. (Color online) (a) BF and (b) DF TEM micrographs for UNCD films annealed at 1000 °C (1 h) after irradiation with 2.245 GeV Au-ions (8.4×10^{13} ions/cm^2). The inset in (a) shows the SAED of the corresponding samples.

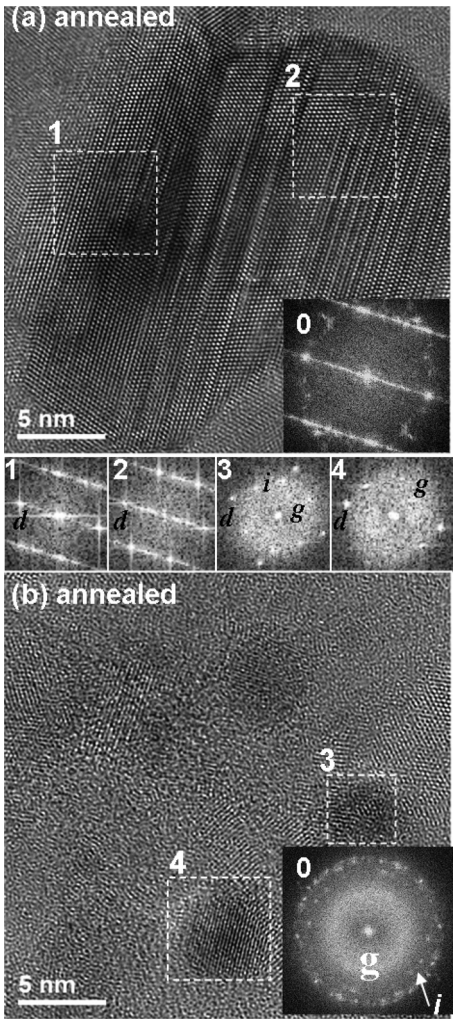

FIG. 9. TEM structure images for UNCD films annealed after irradiation with 2.245 GeV Au-ions (8.4×10^{13} ions/cm^2); (a) typical large-aggregates region and (b) small-grain region along with the FT diffractograms (FT_0) of the corresponding region (insets FT_1–FT_4 show, respectively, the FT diffractograms of the designated areas 1~4 in "a" and "b").

properties of these films is not caused by a change in the nature of the emission sites. Instead, the change is ascribed to the enhancement in electron transport due to the additional interconnecting paths.

The TEM microstructure of the Au-ion irradiated/postannealed $UNCD_{IV}$ films [BF, Fig. 8(a)] is similar to that of the as-irradiated $UNCD_{III}$ films [cf. Fig. 5(a)]. There exist large aggregates that are scarcely distributed over the matrix of ultrasmall diamond grains, which is again inferred by the ring-shaped SAED [inset of Fig. 8(a)]. However, the SAED shows the presence of an additional diffraction ring corresponding to *i-carbons*, which is more clearly illustrated in the linear diffraction pattern (ldp_{II}, Fig. 6). DF images [Fig. 8(b)] corresponding to different parts of the SAED (labeled in green, blue and red circles) confirm the presence of *i-carbons* (green color) along with nanographites (blue color) and large diamond aggregates (red color). Both the *i-carbons* and nanographites are very small in size and are distributed evenly in the samples. The structure image in Fig. 9(a) and the associated FT-diffractogram [FT_0, inset in Fig. 9(a)] for a typical large-aggregate region in the Au-ion irradiated/postannealed UNCD films ($UNCD_{IV}$) show that the size of the diamond clusters in the aggregates increased but the planar defects existing in the diamond clusters are not healed due to such an annealing process. Notably, the diamond clusters are separated in as-irradiated films [cf. Fig. 7(a)] whereas they coalesce into large single diamond grains in the postannealed films [Fig. 9(a)]. The materials located between the clusters were converted into diamonds and were merged into the clusters. Moreover, the structure image for the nanograin region [Fig. 9(b)] shows that the size of the nanodiamond grains has decreased slightly, as illustrated in area 3 [FT_3, Fig. 9(b)]. The FT diffractogram of the whole region in Fig. 9(b) (FT_0, inset) also shows the presence of a diffused ring, which corresponds to nanographites (or amorphous carbons), along with the diffraction spots corresponding to randomly oriented nanodiamond grains. A detailed analysis indicates, again, the presence of diffraction spots corresponding to *i-carbons* (indicated by an arrow). Such an observation implies that the *i-carbons* are most probably transformed from nanographites (or nanosized diamond grains) during the postannealing process.

The sp^3-bonds are very strong, and the diamond material is so stable that even postannealing at 1000 °C can hardly induce modifications of the granular structure of the materials, i.e., no coarsening of the diamond can be induced via such a postannealing process. The phenomenon wherein Au-ion irradiation can induce the formation of large aggregates is very unusual. The thermal spike along the trajectory of heavy ions might induce the melting and recrystallization processes for metallic materials with a relatively low melting point,[25,26] but it is unlikely to happen for diamond materials with an extremely high melting point (3550 °C). There must be some other mechanism that proceeds at lower temperatures. It has been proposed that[27] the formation of ultrananocrystalline grains in UNCD is due to the encapsulation of a layer of hydrocarbons on the surface of the diamond clusters that prevents the active carbon species in the plasma (e.g., C_2) to attach onto diamond clusters to enlarge them. With such an assumption, the removal of the encapsulating hydrocarbons can potentially induce the coalescence of nanosized diamond clusters. Therefore, a possible explanation for the induction of large aggregates due to Au-ion irradiation is proposed as follows: (i) the incident Au-ions disintegrate the hydrocarbons, (ii) the atomic carbons thus formed attach to the nanosized diamond clusters whereas the atomic hydrogen thus formed diffuses away, and (iii) the adjacent diamond clusters then coalesce to form large aggregates. Such processes are facilitated by the presence of the thermal spike produced by the Au-ion irradiation.

The coalescence of nanodiamond clusters into large single-crystallike grains does not seem to be the prime factor that alters the EFE properties of the Au-ion irradiated/postannealed UNCD films because the clusters are only scarcely distributed. On the contrary, the formation of nanographites along the interface region between the large aggregates and the UNCD grains is presumed to be the main factor that alters the EFE properties of the materials. Such a model is schematically illustrated in Fig. 10. The transformed *i-carbons* from nanographites (or nanodiamond grains), which eliminated the interconnected conduction path, are presumed to be the main cause for the degradation of the EFE behaviors of the UNCD films due to the postannealing process.

The phenomenon that heavy ion irradiation enhances the EFE properties of UNCD films has also been observed for 100 MeV Ag^{9+}-ion irradiation.[28] In which study, only a 5×10^{11} ions/cm^2 fluence of 100 MeV Ag^{9+}-ion irradiation decreased the turn-on field by more than 50% and increased the EFE current density by about three orders of magnitude. In this study, 2.245 GeV Au-ion irradiation (8.4×10^{13} ions/cm^2) lowered the turn-on field needed to induce

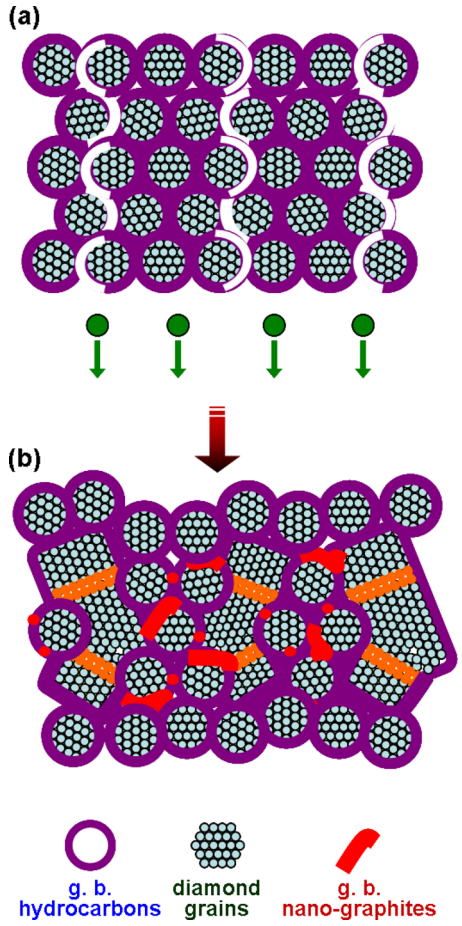

FIG. 10. (Color online) Schematics of the granular structure of UNCD films (a) before and (b) after the heavy ion irradiation process showing the formation of large aggregates and nanographites along the interfacial regions.

the EFE process from 30.0 V/μm to 11.6 V/μm and raised the EFE current density by three to four orders of magnitude (from 1.0×10^{-4} to 1.5 mA/cm^2 for a 20 V/μm applied field). However, the ion fluence required to induce such a large improvement is two orders of magnitude larger than the critical fluence needed in the 100 MeV Ag^{9+}-ion irradiation case. To understand the cause for such a large difference in ion irradiation effects, the ion irradiation characteristics for these ions in UNCD were simulated using the SRIM package, and the results are listed in Table I. From this table, it is clear that 2.245 GeV Au-ions have a larger electronic energy loss and a smaller nuclear energy loss compared to that of 100 MeV Ag^{9+}-ions. Moreover, the SRIM calculation indicates that 2.245 GeV Au-ions can only produce 0.009 vacancies/Å/ion and deposit only 2.5 eV/Å/ion to the diamond lattices; these numbers are smaller than those for 100 MeV Ag^{9+}-ions (0.03 vacancies/Å/ion and 8 eV/Å/ion). Apparently, the ions

TABLE I. SRIM simulation results for energy loss, range, and straggling of Ag- and Au-ions in diamond.

Ions	Electronic energy loss (eV/nm)	Nuclear energy loss (eV/nm)	Projected range (μm)	Longitudinal straggling	Lateral straggling (nm)
100 MeV Ag^{9+}	2.207×10^4	93.71	7.6	229 nm	227
2.245 GeV Au	3.357×10^4	29.16	66.0	1.92 μm	409

that can deposit a larger energy into the diamond lattices are more efficient at inducing the phase transformation process, forming nanographites and enhancing the EFE properties for UNCD films.

IV. CONCLUSION

The effect of Au-ion irradiation at various fluences on the EFE properties of the UNCD films was investigated. Au-ion irradiation with an energy of 2.245 GeV and a fluence of around 8.4×10^{13} ions/cm^2 is required to induce large improvements in the EFE properties of the films. A TEM examination revealed that the prime factor in improving the EFE properties of UNCD films by Au-ion irradiation is the formation of nanographites along the trajectory of the irradiating ions. The induction of grain growth processes, which form large aggregates of UNCD clusters, insignificantly degraded the EFE properties of the films. It is presumed that the proportion of large aggregates was small and scarcely distributed such that they are not blocking the interconnected path for electron transport. Postannealing of the Au-ion irradiated films at 1000 °C (1 h) induced a phase transformation of nanographites (or nanodiamond grains) into *i-carbons* and slightly degraded the EFE properties of the films. However, the resulting EFE behavior is still markedly superior to that of the pristine UNCD films.

ACKNOWLEDGMENTS

Financial support by the National Science Council, Republic of China through Project No. NSC99-2119-M-032-003-MY2 is gratefully acknowledged by the authors. We acknowledge Dr. Christina Trautmann and the Materials Research Group of GSI, Darmstadt for their support during gigaelectron volt irradiation at the XO beamline of the UNILAC.

[1]F. J. Himpsel, J. A. Knapp, J. A. VanVecten, and D. E. Eastman, Phys. Rev. B **20**, 624 (1979).
[2]W. Zhu, G. P. Kochanski, and S. Jin, Science **282**, 1471 (1998).
[3]B. Dischler, C. Wild, W. Müller-Sebert, and P. Koidl, Physica B **185**, 217 (1993).
[4]E. J. Correa, Y. Wu, J. G. Wen, R. Chandrasekharan, and M. A. Shannon, J. Appl. Phys. **102**, 113706 (2007).
[5]Sh. Michaelson, O. Ternyak, R. Akhvlediani, A. Hoffman, A. Lafosse, R. Azria, O. A. Williams, and D. M. Gruen, J. Appl. Phys. **102**, 113516 (2007).
[6]C. J. Tang, M. A. Neto, M. J. Soares, A. J. S. Fernandes, A. J. Neves, and J. Grácio, Thin Solid Films **515**, 3539 (2007).
[7]P. W. May, W. J. Ludlow, M. Hannaway, P. J. Heard, J. A. Smith, and K. N. Rosser, Chem. Phys. Lett. **446**, 103 (2007).
[8]S. G. Wang, Q. Zhang, S. F. Yoon, J. Ahn, Q. Wang, Q. Zhou, and D. J. Yang, Phys. Status Solidi A **193**, 546 (2002).
[9]K. H. Wu, E. G. Wang, Z. X. Cao, Z. L. Wang, and X. Jiang, J. Appl. Phys. **88**, 2967 (2000).
[10]S. Prawer and R. Kalish, Phys. Rev. B **51**, 15711 (1995).
[11]J. Krauser J.-H. Zollondz, A. Weidinger, and C. Trautmann, J. Appl. Phys. **94**, 1959 (2003).
[12]N. Koenigsfeld, H. Hofsass, D. Schwen, A. Weidinger, C. Trautmann, and R. Kalish, Diamond Relat. Mater. **12**, 469 (2003).
[13]S. Prawer, A. Hoffman, and R. Kalish, Appl. Phys. Lett. **57**, 2187 (1990).
[14]W. Zhu, G. P. Kochanski, S. Jin, L. Seibles, D. C. Jacobson, M. McCormac, and A. E. White, Appl. Phys. Lett. **67**, 1157 (1995).
[15]N. Dilawar, R. Kapil, V. D. Vankar, D. K. Avasthi, D. Kabiraj, and G. K. Mehta, Thin Solid Films **305**, 88 (1997).
[16]A. Dunlop, G. Jaskierowicz, P. M. Ossi, and S. Della-Negra, Phys. Rev. B **76**, 155403 (2007).
[17]P. T. Pandey, G. L. Sharma, D. K. Avasthi, and V. D. Vankar, Vacuum **72**, 297 (2004).
[18]P. M. Koinkar, R. S. Khairnar, S. A. Khan, R. P. Gupta, D. K. Avasthi, and M. A. More, Nucl. Instrum. Methods **B244**, 217 (2006).
[19]J. F. Ziegler, J. P. Biersack, and U. Littmark, *The Stopping and Ranges of Ions in Solids* (Pergamon, New York, 1985).
[20]R. H. Fowler and L. Nordheim, Proc. R. Soc. London, Ser. A **119**, 173 (1928).
[21]Z. Sun, J. R. Shi, B. K. Tay, and S. P. Lau, Diamond Relat. Mater. **9**, 1979 (2000).
[22]A. C. Ferrari and J. Robertson, Phys. Rev. B **63**, 121405 (2001).
[23]J. Michler, Y. Von Kaenel, J. Stiegler, and E. Blank, J. Appl. Phys. **83**, 187 (1998).
[24]A. C. Ferrari and J. Robertson, Phys. Rev. B **61**, 14095 (2000).
[25]F. F. Komarov, Phys. Usp. **46**, 1253 (2003).
[26]T. A. Belykh, A. L. Gorodishchensky, L. A. Kazak, V. E. Semyannikov, and A. R. Urmanov, Nucl. Instrum. Methods **B51**, 242 (1990).
[27]C. S. Wang, H. C. Chen, H. F. Cheng, and I. N. Lin, J. Appl. Phys. **107**, 034304 (2010).
[28]H. C. Chen, U. Palnitkar, W. F. Pong, I. N. Lin, A. P. Singh, and R. Kumar, J. Appl. Phys. **105**, 083707 (2009).